Effect of Copolymer Architecture on the Micellization and Gelation of Aqueous Solutions of Copolymers of Ethylene Oxide and Styrene Oxide

Silvia Barbosa,* Mohammad Arif Cheema,† Pablo Taboada, and Víctor Mosquera*

Grupo de Sistemas Complejos, Laboratorio de Física de Coloides y Polímeros, Departamento de Física de la Materia Condensada. Facultad de Física, Universidad de Santiago de Compostela 15782, Spain

Received: May 7, 2007; In Final Form: July 6, 2007

The micellar properties and solubilization capacity of poorly water soluble drugs of several micellar and gel solutions of diblock and triblock copolymers of styrene oxide/ethylene oxide have been measured and compared with block copolymers of butylene oxide/ethylene oxide, showing that the solubilization capacity of the styrene oxide block is approximately four times that of a butylenes oxide block for dilute solutions. To continue establishing the correlation between micellar characteristics and solubilization capacity, we have found it interesting to compare the micellar and gelation properties of the diblock and triblock copolymers PSO_{10}-PEO_{135} and $PEO_{69}PSO_8PEO_{69}$ (subindexes are the number-average block lengths), with different architecture but similar average block lengths. Surface tension measurements allowed the determination of the critical micelle concentrations at several temperatures and, so, to calculate standard enthalpies of micellization. Static and dynamic light scattering data permitted us to determine micellar parameters and to obtain qualitatively the extent of hydration of the copolymer micelle. A tube inversion method was used to define the mobile−immobile (soft−hard gel) phase boundary. To refine the phase diagram and observe the existence of additional phases, rheological measurements were done. The results are in good agreement with previous values published for PSO_nPEO_m and $PEO_mPSO_nPEO_m$ copolymers.

Introduction

The aggregation and gelation of diblock and triblock copolymers of polyoxyalkylene block coplymer in aqueous solution have been extensively studied, as indicated by the large number of reviews and articles found in literature.[1−10] Variation of hydrophobic block, block length, and architecture allows close control of their physicochemical properties. The most familiar copolymers of this type are those whose hydrophobic block is formed by units of oxypropylene ($-OCH_2CH(CH_3)$, denoted as PPO) or 1,2-oxybutylene ($-OCH_2CH(C_2H_5)$, denoted as PBO), commercially available by BASF[11] and Dow Chemical Co.,[12] respectively. The ratio of logarithm critical micelle concentrations (log(cmc/molar)) for these blocks is PPO:PBO = 1:6,[4] which gives the hydrophobic factor and is proportional to the standard free energy of micellization. Less attention has been paid to the association behavior of copolymers with a hydrophobic block formed by oxyphenylethylene units ($-OCH_2CH(C_6H_5)$) prepared from styrene oxide (denoted as PSO), recently released to the market by Goldschimdt AG.[13] The hydrophobicity ratio of a styrene oxide unit compared to a butylene oxide one lies PBO:PSO = 1:2.[4] Aqueous solutions of this class of block copolymers also form aggregates in dilute solutions and their concentrated micellar gel solutions.[1−3,6,7] A recent review summarizes the physicochemical properties of these copolymers in terms of copolymer architecture, hydrophilic and hydrophobic block length, concentration, and temperature and compares them to structurally related propylene oxide and butylene oxide block copolymers.[14] It has been also demonstrated that this class of copolymers is particularly efficient in the solubilization of certain very hydrophobic aromatic drugs in aqueous solution.[15,16] In a recent work[16] we have measured the solubilization capacity of several micellar and gel solutions of diblock and triblock copolymers of styrene oxide/ethylene oxide and compared them with block copolymers of butylene oxide/ethylene oxide, showing that the capacity of the styrene oxide block is approximately four times that of a butylene oxide block for dilute solutions. In this present paper, we focus on the physicochemical properties of two of the styrene oxide/ethylene oxide block copolymers, $PSO_{10}PEO_{135}$ and $PEO_{69}PSO_8PEO_{69}$, one of them (the diblock) used in this previous study, where the subscripts denote the length of each block, in order to obtain the micellar and gelation characteristic parameters. Thus, we study the extent of micellization, micellar composition, structure and rheological behavior for both block copolymers by surface tension, light scattering, and rheometry measurements as a function of temperature in both dilute and concentrated regimes. These two block copolymers have been chosen because of their different architecture but similar total average block lengths. Nevertheless, one should bear in mind that the PSO blocks of the triblock copolymers loop in the micelle core, so they would act effectively as a PSO_4PEO_{69}. The quantities of the derived magnitudes are compared and correlated with those of previously synthesized structurally related block copolymers.

2. Experimental Section

2.1. Materials. Copolymers $PSO_{10}PEO_{135}$ and $PEO_{69}PSO_8$-PEO_{69} were prepared by sequential oxyanionic polymerization of styrene oxide followed by ethylene oxide starting from a monofunctional or difunctional initiator to form the hydrophobic block as described in detail by Crothers et al.[16] Table 1 shows the molecular characteristics of the copolymers.

* To whom correspondence should be addressed. Telephone: 0034981563100, ext.14056. Fax: 0034981520676. E-mail: fmsilvia@usc.es (S.B.); fmvictor@usc.es (V.M.).

† Permanent address: Department of Chemistry, Quaid-i-Azam University Islamabad, 45320, Pakistan.

10.1021/jp073481i CCC: $37.00
Published on Web 08/24/2007

TABLE 1: Molecular Characteristics of the Copolymer Samples[a]

samples	M_n/(g mol^{-1}) (NMR)	wt % PEO	M_w/M_n (GPC)	M_w/(g mol^{-1})
$PSO_{10}PEO_{135}$	7140	83	1.04	7430
$PEO_{69}PSO_8PEO_{69}$	7030	86	1.05	7380

[a] Estimated uncertainty: M_n to ±3%; wt % PEO ± 1%; M_w/M_n to ±0.01. M_w calculated from M_n and M_w/M_n.

2.2. Surface Tension. Surface tensions, γ, of dilute aqueous solutions were measured by the Whilhelmy plate method using a Krüss K-12 instrument equipped with a processor to acquire the data automatically and with water bath temperature control. The solutions were measured at three temperatures of 20, 30, and 40 °C. The plate was cleaned by washing with doubly distilled water followed by heating in an alcohol flame. A stock solution was prepared with distilled water and diluted as required. In the measurements, a solution was equilibrated at 20 °C prior to measurement, and then γ was measured every 15 min until consistent readings were obtained. Thereafter, the temperature was raised and the procedure repeated. The accuracy of the measurement was checked by frequent determination of the surface tension of pure water.

2.3 Light Scattering. Dynamic and static light scattering (DLS and SLS) intensities were measured for solutions at temperatures in the range of 20−50 °C by means of an ALV-5000F (ALV-GmbH, Germany) instrument with vertically polarized incident light of wavelength $\lambda = 532$ nm supplied by a continuous wave (CW) diode-pumped Nd:YAG solid-state laser supplied by Coherent Inc., CA, and operated at 400 mW. The intensity scale was calibrated against scattering from toluene. Measurements were made at the scattering angle of 90° to the incident beam. Solutions were equilibrated at each chosen temperature for 30 min before making a measurement. The experiment duration was in the range of 5−15 min, and each experiment was repeated two or more times. To eliminate dust, samples were filtered through Millipore Millex filters (Triton free, 0.22 μm porosity).

The correlation functions from DLS were analyzed by the CONTIN method to obtain intensity distributions of decay rates (Γ).[17] Integration over intensity of the decay rate distributions gave the intensity-weighted average of D_{app}. Values of the apparent hydrodynamic radius, $r_{h,app}$, were calculated from the Stokes−Einstein equation

$$r_{h,app} = kT/(6\pi\eta D_{app}) \quad (1)$$

where k is the Boltzmann constant and η is the viscosity of water at the thermodynamic temperature, T.

The basis for analysis of SLS was the Debye equation

$$K^*c/(I - I_s) = 1/M_w + 2A_2c + ... \quad (2)$$

where I is the intensity of light scattering from solution relative to that from toluene, I_s, c is the concentration (g dm^{-3}), M_w is the mass-average molar mass of the solute, A_2 is the second virial coefficient (higher coefficients being neglected), and K^* is the appropriate optical constant. Values of the specific refractive index increment, dn/dc, and its temperature increment were taken from previous reports.[1,2] The possible effect of the different refractive indices of the blocks on the derived molar masses of micelles has been found to be negligible.[6] Other quantities used were the Raleigh ratio of toluene for vertically polarized light, $R_v = 2.57 \times 10^{-5}[1 + 3.68 \times 10^{-3}(t - 25)]$ cm^{-1} (t in °C) and the refractive index of toluene, $n = 1.4969-[1-5.7 \times 10^{-4}(t - 20)]$.[18]

In practice, the Debye equation taken to the second term, A_2, could not be used to analyze SLS data as micellar interaction causes curvature of the Debye plot across the concentration range investigated. The fitting procedure used was based on scattering theory for hard spheres,[19] whereby the interparticle structure factor (S) in the equation

$$K^*c/(I - I_s) = 1/SM_w \quad (3)$$

was approximated by

$$1/S = [(1 + 2\phi)^2 - \phi^2(4\phi - \phi^2)]\,(1 - \phi)^{-4} \quad (4)$$

where ϕ is the volume fraction of equivalent uniform spheres. Values of ϕ were conveniently calculated by applying a thermodynamic expansion factor $\delta_t = \upsilon_t/\upsilon_a$, where υ_t is the thermodynamic volume of a micelle (i.e., one-eighth of the volume, u, excluded by one micelle to another) and υ_a is the anhydrous volume of a micelle ($\upsilon_a = M_w/N_A\rho_a$, where N_A is Avogadro's constant and ρ_a is the liquid density of the copolymer solute calculated assuming mass additivity of specific volumes).[20] The method is equivalent to using the virial expansion for the structure factor of effective hard spheres taken to its seventh term[19b] but requires just two adjustable parameters, i.e., M_w and δ_t.

2.4. Tube Inversion. The mobility of solutions was explored using a inverted-tube test. Solutions (concentration range of 20−80 wt %) were prepared by weighing copolymer and water into small tubes (10 mm in diameter) and were mixed in the mobile state before being stored at low temperature for seveal days ($T \approx 5$ °C). Tubes containing 0.5 cm^3 solution were immersed in a water bath, which was heated at a heating/cooling rate of 0.2 °C min^{-1} from 5 to 90 °C. The change from a mobile to an immobile system (or vice versa) was determined by inverting the tube at 1 min intervals.

2.5. Rheometry. The rheological properties of the samples were determined using a Bohlin CS10 rheometer with water bath temperature control. Couette geometry (bob, 24.5 mm in diameter, 27 mm in height; cup, 26.5 mm in diameter, 29 mm in height) was used, with a 2.5 cm^3 sample being added to the cup in the mobile state. Samples of very high modulus were investigated using cone-and-plate geometry (diameter of 40 mm, angle of 4°). A solvent trap maintained a water-saturated atmosphere around the cells. Frequency scans of storage (G') and loss (G'') moduli were recorded for selected copolymer concentrations and temperatures with the instrument in oscillatory shear mode and with the strain amplitude (A) maintained at a low value ($A < 0.5\%$) by means of autostress facility of the Bohlin software. This ensured that measurements of G' and G'' were in the linear viscoelastic region. Temperature scans were recorded for selected copolymer concentrations at a frequency 1 Hz. The samples were heated at ca. 0.5 °C in the range of 5−80 °C. Measurements on solutions of low modulus ($G' = 1-10$ Pa), which fell outside the range for satisfactory autostress feedback were rejected.

3. Results and Discussion

3.1. cmc Determination and Surface Properties. Clouding of aqueous solutions of the copolymers in the concentration range of 10−80 wt % were investigated over the temperature range of 5 to 90 °C. All solutions remained clear under these conditions.

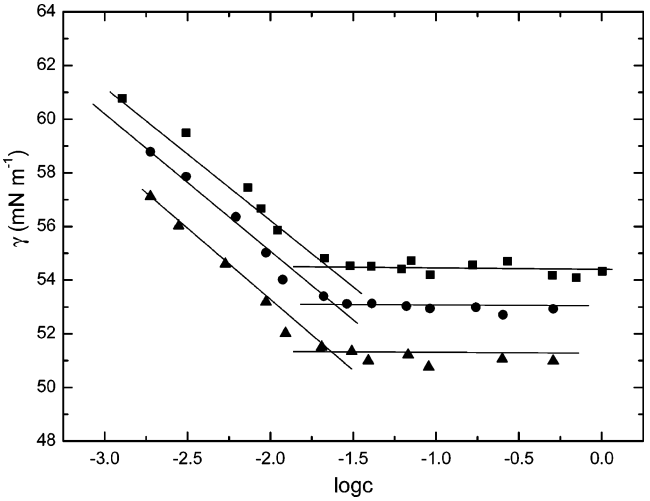

Figure 1. Surface tension (γ) vs logarithm of concentration (g dm^{-3}) for aqueous solutions of copolymer $PSO_{10}PEO_{135}$ at (■) 20, (●) 30, and (▲) 40 °C.

TABLE 2: Critical Micelle Concentration, cmc, Surface Tensions at the cmc, γ_{cmc}, Excess Concentration, Γ, and Area Per Molecule, *A*, for Aqueous Solutions of Copolymers $PSO_{10}PEO_{135}$ and $PEO_{69}PSO_8PEO_{69}$

	T/°C	cmc/ (g dm^{-3})	γ_{cmc}/ (mN m^{-1})	$10^{-10}\Gamma$/ (mol cm^{-2})	*A*/(nm^2)
$PSO_{10}PEO_{135}$	20	0.023	54.5	4.6	3.6
	30	0.023	53.1	4.7	3.5
	40	0.024	51.3	4.8	3.4
$PEO_{69}PSO_8PEO_{69}$	20	0.21	55.5	2.9	5.7
	30	0.14	53.9	3.2	5.2
	40	0.10	51.7	3.7	4.4

Plots of surface tension against logarithm of concentration for aqueous solutions of $PSO_{10}PEO_{135}$ copolymer in the temperature range of 20−40 °C are shown in Figure 1. A similar plot was obtained for the triblock one (not shown). The concentration at which the surface tension departed from its steady value served to define the value of log(cmc) to ±0.05. Values are listed in Table 2 for both copolymers, together with values of the surface tension at the cmc.

It can be observed that the cmc of the diblock copolymer is insensitive to temperature but not for the triblock, for which it significantly decreases. Also, it can be observed that the triblock copolymer has cmc values approximately 1 order of magnitude higher than the diblock copolymer. The effect is originated by the entropy of the triblock chains constrained by two block junctions in the core−shell interface of the aggregate, compared with only one constraint for the diblock chain. If the cmcs of copolymers $PSO_{10}PEO_{135}$ and $PEO_{69}PSO_8PEO_{69}$ at 20 °C, 0.018 and 0.51 g dm^{-3}, respectively, are compared with those of the structurally related copolymers $PEO_{45}PSO_{10}$ and $PEO_{82}PSO_8$-PEO_{82},[1,2] it can be observed that the longer the EO block length the more hydrophilic the copolymer becomes. It has been proposed by Booth et al. that the dependence of the cmc on the number of EO units in a copolymer (ν) is small for styrene oxide based block copolymers, unless the hydrophobic SO length is short, e.g., equal to or less than 10.[21] Thus, within a series of copolymers and bearing in mind that our two copolymers possess short hydrophobic blocks, it is desirable to account and correct for the cmc variation with EO block length. Comparison of the cmc values for the present copolymers with those of other diblock and triblock PEO/PSO copolymers as a function of hydrophobic block length is made in Figure 2.

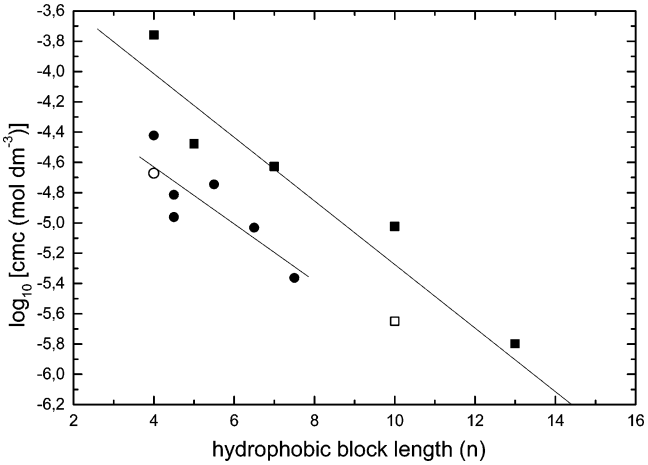

Figure 2. Logarithm of cmc (mol dm^{-3}) versus hydrophobic block length (*n*) for aqueous solutions at 30 °C of diblock copolymers (■) PEO_mPSO_n and triblock copolymers (●) $PEO_mPSO_nPEO_m$ plotted using half-length *n*/2 (from refs 4 and 14). Open symbols correspond to the copolymers studied in the present work.

Triblock copolymers are plotted as if they were diblocks with hydrophobic length *n*/2, since their effective block length is half of a related diblock due to looping of PSO block in the micelle core.

Previous studies[14] have shown that the rate of variation of the cmc with ν is d log(cmc)/dν = 0.004 ± 0.002, where ν = 2*m*, obtained from Pluronics $PEO_mPPO_nPEO_m$ block copolymers with EO block ranging from 13 to 132 units. Assuming that this variation is also followed by SO block copolymers, an adjustment of 0.004 ($x - m$) was used to correct each value for a change in EO-block length, where x is the assumed average block length x = 100, this being a rough average taken from ref 14. As observed in Figure 2, cmcs for $PSO_{10}PEO_{135}$ and $PEO_{69}PSO_8PEO_{69}$ are in the same line as other previously reported PEO/PSO block copolymers, following the expected trend of cmc dependence with PSO-block length.[14]

On the other hand, values of the cmc of the diblock copolymer were independent of temperature over the range examined: cmc ∼ 0.023 g dm^{-3}. This insensitivity of the cmc to temperature means that the standard enthalpy of micellization ($\Delta_{mic}H°$) is approximately zero over the temperature range used in these measurements, as shown for other similar PEO−PSO diblocks,[1,14] or other diblock copolymers bearing a more hydrophobic block.[22,23] This effect has been attributed to the SO blocks being tightly coiled in the dispersed unimer state (called unimolecular micelle),[24] so that the hydrophobic interaction with water is small, as discussed in detail in ref 15. In the case of the triblock copolymer, an apparent value of the standard enthalpy of micellization can be obtained through the standard van't Hoff enthalpy of micellization, $\Delta_{mic}H_{\nu H} = RT[d(\ln(cmc))/d(1/T)]$, as described in detail elsewhere,[25] correctly describing the variation of the cmc with temperature. In our case, for copolymer PEO_{69}-PSO_8PEO_{69} we derive a value of $\Delta_{mic}H_{\nu H}$ of 28 kJ mol^{-1} at 30 °C, in certain fair agreement with the calorimetric data at the same temperature (10 kJ mol^{-1}).[2] The difference between both values has been considered as a consequence of the distribution of block chain lengths, i.e., the van't Hoff enthalpy related to the most readably micellized species and the enthalpy of micellization from calorimetry related to the whole sample.[26] The nonnull value of standard enthalpy of micellization and the higher cmc values of the triblock copolymer can be attributed to its shorter effective block length due to looping of the PSO blocks in the micellar core, as commented before.

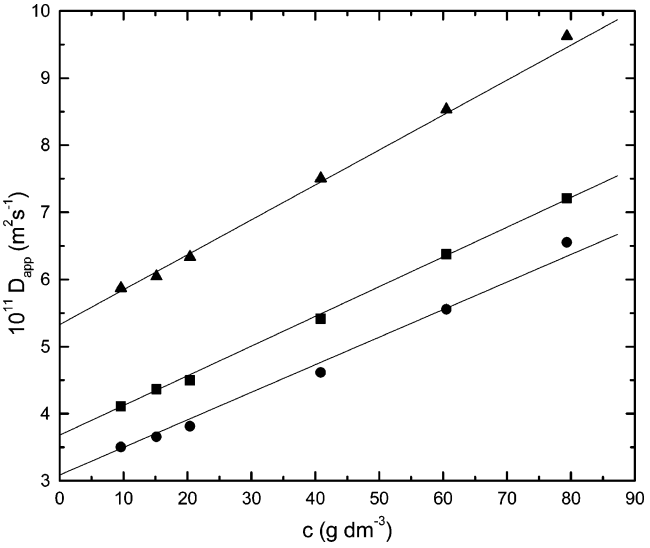

Figure 3. Concentration dependence of apparent diffusion coefficients for aqueous micellar solutions of copolymer $PEO_{69}PSO_8PEO_{69}$ at (●) 20, (■) 30, and (▲) 40 °C.

From the slopes of the surface tension curves below the cmc, the excess surface concentration (Γ) of non-ionic copolymer at the air−water interface can be calculated by using the Gibbs adsorption isotherm:[27]

$$\Gamma = -\frac{1}{4.606RT}\frac{d\gamma}{d\log m} \quad (5)$$

where R is the gas constant, T is the temperature in Kelvin, γ is the surface tension, and m is the concentration expressed in mol dm^{-3}. Within the assumption that the concentration of solute in solution is negligible compared to its concentration at the interface, the values of Γ correspond to the areas per molecule at the surface monolayer, A:

$$A = \frac{1}{\Gamma N_A} \quad (6)$$

where N_A is the Avogadro number.

As observed in Table 2, results obtained for Γ and A are almost independent from temperature for copolymer PSO_{10}-PEO_{135}, whereas for the triblock A decreases as the temperature increases. For the triblock copolymer A decreases with temperature; meanwhile for diblock it remains nearly unchanged as a consequence of the compact packing of the copolymer chains even in the unimer state. The diminution from the triblock arises from (a) the increase of thermal motions in the hydrophilic chains and (b) their dehydration as the temperature rises.[28,29] Comparison of the surface parameters of the diblock copolymer with its counterpart $PEO_{45}PSO_{10}$ (with values of 4.0×10^{-10} mol cm^{-2} and 4.1 nm^2 for Γ and A, respectively, at 30 °C) shows that the lengthening of the hydrophobic chain involves a larger coverage of the surface area.

3.2. Micelle Properties: Light scattering measurements were made for copolymer solutions at 20, 30, and 40 °C and at concentrations in the range of 5−80 g/L. Intensity fraction distributions of log $r_{h,app}$ for both copolymers obtained from DLS (not shown) were single narrow peaks, indicative of a closed association process, and similar to those found previously for other EO/SO copolymers at different temperatures.[1,2]

Plots of the apparent diffusion coefficients, D_{app}, for the triblock copolymer are depicted in Figure 3. A similar graph was obtained for the diblock (not shown) The intercepts at $c = 0$ of these linear plots by using the Stokes−Einstein relation, eq 1, allows determination of the hydrodynamic radius, r_h, values listed in Table 3. Within experimental error, temperature had very little effect on r_h, as is usually found for block copoly(oxyalkylenes).[4,30] The positive slopes in Figure 3 are consistent with spherical micelles effectively interacting as hard spheres.[9] This behavior is usually accommodated by introducing a diffusion second virial coefficient, k_d, in the equation of the straight line in terms of D_{app}

$$D_{app} = D(1 + k_d c + ...) \quad (7)$$

The coefficient k_d is related to the thermodynamic second virial coefficient A_2 by[31]

$$k_d = 2A_2M_w - k_f - 2\upsilon \quad (8)$$

where k_f is the friction coefficient, M_w is the mass-average molar mass of the solute, and υ is the specific volume of the micelles in solution. As seen from Figure 3, the positive term in eq 7 is dominant for both copolymers, relating A_2 to the effective hard-sphere volume of the micelles, υ_{hs} ($A_2 = 4N_A\upsilon_{hs}/M_w^2$, where N_A is Avogadro's constant). Flory[32] shows that the first term depends on the ratio υ_{hs}/M_w. We have no direct measure of υ_{hs}, but it will be closely related to the hydrodynamic volume, as we shall see ahead.

The Debye equation[2] was the basis of the analysis of SLS from solutions at three temperatures, 20, 30, and 40 °C. For the present micellar solutions, the dissymmetry of light scattering from solution at 45 and 135°, (I_{45}/I_{135}), in SLS was shown to be 1.01 or less, which is consistent with micelles with small radii of gyration and corresponds to a correction factor less than 1% to the 90° scattering intensity;[33] a maximum value of r_g = 9.19 and 5.3 nm for $PSO_{10}PEO_{135}$ and $PEO_{69}PSO_8PEO_{69}$, respectively, can be estimated from $r_g = 0.775r_h$ (with r_h from Table 3) by treating the micelles as uniform spheres. Consequently scattering intensities measured at 90° were used without correction for intraparticle interference.

Curvature in the Debye plots is illustrated in Figure 4 for $PSO_{10}PEO_{135}$. A similar plot is obtained for $PEO_{69}PSO_8PEO_{69}$ (not shown). The curves drawn through the data points are based on scattering theory for hard spheres, as described in section 2.3.

The values of M_w and δ_t obtained from fitting of experimental data shown in Figure 4 to theory for hard spheres[19] are also

TABLE 3: Micellar Properties for PEO/PSO Block Copolymers in Aqueous Solution[a]

copolymer	T/°C	M_w/(10^5 g mol^{-1})	N_w	δ_t	r_t/(nm)	r_h/(nm)	υ_E/(nm^3)	n_w
$PSO_{10}PEO_{135}$	20	6.0	80	5.0	10.2	11.8	0.49	11
	30	6.6	89	4.5	10.1	11.1	0.35	9
	40	7.3	98	4.3	10.3	10.3	0.33	8
$PEO_{69}PSO_8PEO_{69}$	20	1.3	17	3.6	5.5	6.8	0.58	17
	30	1.4	19	3.5	5.6	6.7	0.54	15
	40	1.6	22	3.3	5.7	6.6	0.50	14

[a] Estimated uncertainty in r_h, ±4%; and M_w and N_w, ±10%.

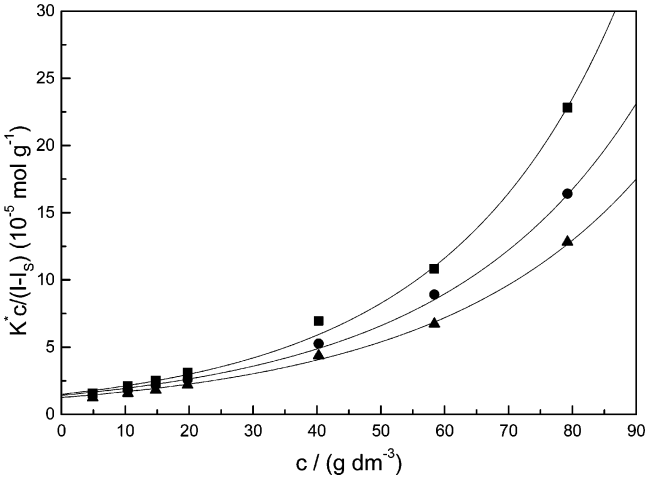

Figure 4. Debye plots for aqueous solutions of $PSO_{10}PEO_{135}$ at different temperatures: (■) 20, (●) 30, and (▲) 40 °C.

listed in Table 3. The mass-average association numbers of the micelles were calculated from (see Table 3)

$$N_w = \frac{M_w(\text{micelle})}{M_w(\text{molecule})} \tag{9}$$

with M_w(molecule) being the mass molecular weight of a single copolymer molecule (taken from Table 1) and M_w(micelle) calculated using values of M_w for the micelles from the intercepts of the Debye plots.

The value of N_w for a given copolymer increases slightly as temperature is increased as expected, since water becomes a poorer solvent for the polyoxyethylene blocks. This is consistent with the effect of temperature in micelles of other copoly(oxyalkylenes).[4,30] From this respect, taking the length of a SO unit to be 0.36 nm per chain unit,[32] the average length of the fully stretched SO_{10} and SO_8 blocks of the diblock and triblock copolymers, respectively, are 3.6 and 2.9 nm. As the central block is looped in the micelle core in the case of the triblock copolymer, the effective length is 1.5 nm. The average core volume (ν_c) and core radius (r_c) can be estimated from the equation

$$\nu_c = (4/3)\pi r_c^3 = n\nu_S N_w \tag{10}$$

where ν_S is the volume of a SO unit

$$\nu_S = M_{w,S}/\rho_s N_A \tag{11}$$

with $M_{w,S} = 120$ g mol^{-1} and $\rho_S = 1.13$ g cm^{-3} being the molar mass of a SO unit and the density of liquid oxystyrene, respectively, assuming spherical micelle cores with no penetration of water. Representative values of N_w of 90 ($PSO_{10}PEO_{135}$) and 20 ($PEO_{69}PSO_8PEO_{69}$) imply core radii of ca. 3.4 and 1.9 nm, respectively, equivalent to fully stretched chains of length 3.6 and 1.7 nm, respectively. Assuming that SO blocks have Poisson distributions, as expected in an ideal polymerization of an alkylene oxide,[32] and given the range of block lengths, we see that spherical (or near-spherical) micelles are possible for both block copolymers, although further stretching of the SO blocks in the core will act against any substantial increase of N_w with temperature. In addition, accordingly with the assumption that micelles have a spherical structure with a liquid-like core[34] free of solvent molecules, we can further evaluate the extent of drainage of the micellar corona. From the reduction of the thermodynamic radius, r_t, by r_c, the thickness of the micellar corona is obviously derived, and, hence, the volume of each water swollen EO unit, ν_E, can be derived from the following relation:

$$(4/3)\pi(r_t^3 - r_c^3) = mN_w\nu_E = \langle L_h \rangle \tag{12}$$

where L_h is the micellar corona thickness and ν_E the volume of each water-swollen EO unit. Values of ν_E are listed in Table 3. Taking into account that the volume of an unswollen liquid EO unit is 0.073 nm^3 and that the volume of water molecule is close to 0.030 nm^3, the number of water molecules associated with each EO unit, n_w, can be estimated (see also Table 3). From these data we can observe that as temperature increases the extent of the corona hydration decreases, as expected, but the level of hydration in the corona remains still important at high temperatures. From this respect, Raman spectroscopy has been used to show that there are six water molecules in the hydration shell of an EO unit: two H-bonded directly to the ether oxygen and four involved in hydrophobic hydration of the hydrophobic part of the unit.[35] The rest will be essentially bulk water, restricted to the corona to some extent, which is determined by the balance of osmotic and dynamic forces in a given situation.

On the other hand, N_w values of both block copolymers were used in order to know if they follow the established dependence of the association number with hydrophobic block length. In particular, the hydrophobic block length dependence for oxystyrene-based block copolymers follows the relationships $N_w \sim (n')^{1.10\pm0.05}$ and $N_w \sim (n')^{0.95\pm0.12}$ for PEO_mPSO_n/PSO_nPEO_m and $PEO_mPSO_nPEO_m$ block copolymers, respectively, with $n' = n - n_{cr}$, n being the hydrophibic block length and n_{cr} the critical hydrophobic length (the minimum hydrophobic block length to enable copolymer association), with values of 1 and 2 for diblock and triblock architectures of PEO/PSO copolymers, respectively.[14] To take into account the effect of the hydrophilic blocks length in this representation, it has been stated very recently[14] that for polyoxyalkylene block copolymers the N_w dependence with EO-block length (m) follows the general scaling law $N_w \sim m^{-0.63\pm0.05}$. In Figure 5, plots of the dependence of the association number accounting for different EO block lengths against the hydrophobic block length are shown for several PEO/PSO block copolymers, including those of the present study. Triblock copolymers are plotted as if they were diblocks with hydrophobic length $n/2$, as stated before. Both present copolymers fit fairly well according to the established scaling relationships as seen in the figure.

3.3. Gel Properties. Solutions of the copolymers (20−80 wt %) were investigated for gel formation using tube inversion experiments. Immobility implies no detectable flow over a period of hours or days. To a good approximation, immobility in the test requires the gel to have a yield stress higher than 30 Pa.[36] Adopting the notation used by Hvidt et al.,[36−38] this immobile phase is referred to as "*hard gel*".

The gel boundaries found for aqueous micellar solutions of copolymers $PSO_{10}PEO_{135}$ and $PEO_{69}PSO_8PEO_{69}$ are shown in Figure 6. There is no low-temperature boundary to the hard gel, a feature attributed to the stability of the micelles of these copolymers in water at low temperatures and consistent with the very low standard micellization enthalpy values of this type of copolymers. Solutions of other copolymers (e.g., PEO_mPBO_n-PEO_m and $PEO_mPPO_nPEO_m$) characteristically have a low-T mobile/immobile boundary as well as a high-T boundary.[4,38] The upper limit of measurement was 90 °C, and the hard gel boundaries cross this limit at ca. 35% (w/v) for $PSO_{10}PEO_{135}$. Beyond these concentrations, the solutions were immobile at all temperatures up to the highest concentration examined (80%

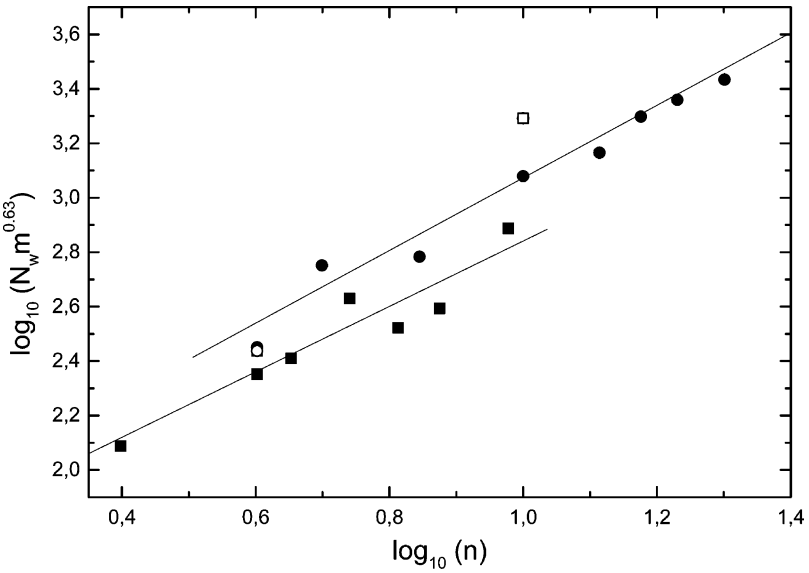

Figure 5. Dependence of association number, N_w, on SO-block length, n, for (■) PEO-PSO and (●) PEO-PSO-PEO block copolymers plotted using half-length $n/2$ at 40 °C (from refs 4 and 14). Open symbols denote copolymer analyzed in the present work.

(w/v)) for this copolymer. In the case of the triblock, the hard gel boundary starts at ca. 24% (w/v) and becomes a fluid regime at temperatures lower than ca. 40 °C, following a profile similar to the copolymer $PEO_{82}PSO_8PEO_{82}$.

Gelation can be understood in terms solvent-swollen spherical micelles filling space as effective hard spheres.[38−40] In this way, it is useful to compare the phase boundaries of copolymers $PEO_{45}PSO_{10}$ and $PSO_{10}PEO_{135}$ as a consequence of the longer EO-block length of the latter (see Figure 6),[1] which excludes larger micelle volumes one to another, as seen for other polyoxyalkylene block copolymers.[41,42] Usually, in considering packing, the relevant parameter is the volume fraction of effective hard spheres, which can be obtained from SLS by means of the thermodynamic volume.

The volume fraction will be

$$\phi \approx \frac{c\delta_t}{10^2\rho_a} \tag{13}$$

where c is the copolymer concentration in percent (w/v). Therefore, for block copolymers in aqueous solution it has been shown that the critical gelation concentration, cgc, at a given temperature can be predicted from micellar properties measured in dilute solution provided that the structure of the gel is known.[43−45] In our case, for PSO_nPEO_m diblock and PEO_m-PSO_nPEO_m triblock, spherical micelles are packed in cubic arrays (face-centered cubic structures for diblock and body-centered structures for triblock).[43,46] The critical values in both cases are as follows: $\phi_c = 0.74$ and 0.68, respectively, and $\rho_a = 1.13$ g cm^{-3} at 30 °C. The values of the cgc calculated from eq 14 in the form

$$\text{cgc} = \frac{10^2\rho_a\phi_c}{\delta_t} \tag{14}$$

are 19% (w/v) for $PSO_{10}PEO_{135}$ and 22% (w/v) for $PEO_{69}PSO_8$-PEO_{69}, which are in reasonable agreement with experiments (see Figure 6).

To get more detailed information about the block copolymer phases and the effect of corona length on these, we have performed rheology measurements of the diblock copolymer $PSO_{10}PEO_{135}$. In describing complex systems of this type, we adopt Hvidt's et al. notation, as previously commented.[36,38] They have used yield stress (σ_y) and modulus (storage and loss, G' and G'') to define three convenient subdivisions of the range of behaviors observed: immobile hard gel (high σ_y and G', $G' > G''$), mobile soft gel (low σ_y and G', $G' > G''$), and mobile sol (null σ_y and very low G', $G' < G''$).

Temperature scans of storage and loss moduli were used to explore the rheological behavior of micellar solutions of the diblock copolymer at concentrations below and above the critical gel concentration in order to complete its phase diagram. Figure 7a shows an example of a temperature scan of the logarithm of elastic modulus for a concentrated solution above the cgc for copolymer $PSO_{10}PEO_{135}$. On the basis of a critical value of $G' = 1$ kPa for a hard gel, the 23% (w/v) is a hard gel up to $T \approx 68$ °C, with a maximum value of $G' \approx 16$ kPa, being $G' > G''$ throughout the whole experiment. In Figure 7b, temperature scans of G' for solutions of the same copolymer at concentrations below the hard-gel boundary (4−16% (w/v)) are also shown. Using the conditions described above, at temperatures at which G' (1 Hz) exceeds 10 Pa, the solutions are soft gels, otherwise sols. As illustrated in Figure 7c, within the region of raised modulus G' was higher than G'', which justifies the convenient term "soft gel" for the fluid in order to distinguish it from sol.

In general, for a given copolymer concentration the G' value increases at low temperature and decreases at high temperatures. In addition, the maximum value of G' also increases with concentration. As discussed elsewhere,[47−49] for aqueous gel solutions of copoly(oxyalkylene)s of various block architectures the onset of gelation and its increase at low temperature is associated with an increase in the extent of aggregation (i.e., an increase in the effective volume fraction of micelles in solution). A decrease in G' with increases in temperature at high temperatures is associated with the water becoming a worse solvent for polyoxyethylene, resulting in a compression of the EO-block corona and, thereby, a decrease in the effective micellar volume fraction.

A phase diagram of the regions of sol, soft gel, and hard gel defined by rheometry and tube inversion of copolymer PSO_{10}-PEO_{135} are shown in Figure 8. These sol−gel diagrams follow

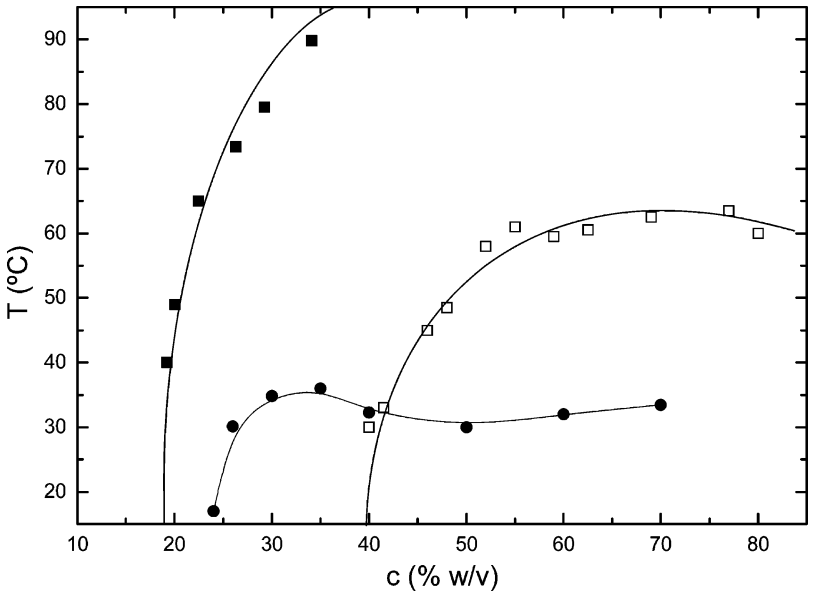

Figure 6. Hard gel boundaries from tube inversion for (■) $PSO_{10}PEO_{135}$, (●) $PEO_{69}PSO_8PEO_{69}$, and, for comparison, (□) $PEO_{45}PSO_{10}$ in aqueous solution.

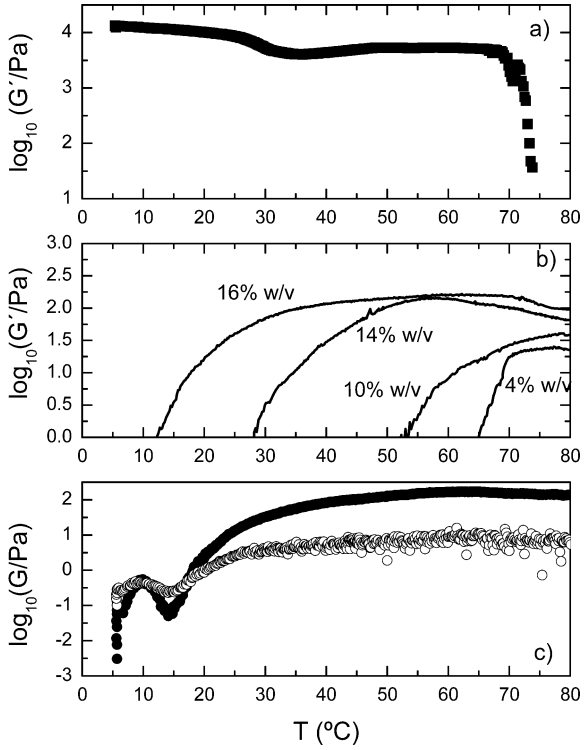

Figure 7. Aqueous solutions of copolymer $PSO_{10}PEO_{135}$: (a) temperature dependence of log(G') for aqueous hard gel at 23% (w/v), frequency of $f = 1$ Hz, and strain amplitude of $A = 0.5\%$; (b) temperature dependence of log(G') at concentrations below the hard-gel boundary, at $f = 1$ Hz and $A = 0.5\%$; (c) temperature dependence of storage (G') (●) and loss (G'') (○) moduli at 16% (w/v), $f = 1$ Hz, and $A = 0.5\%$.

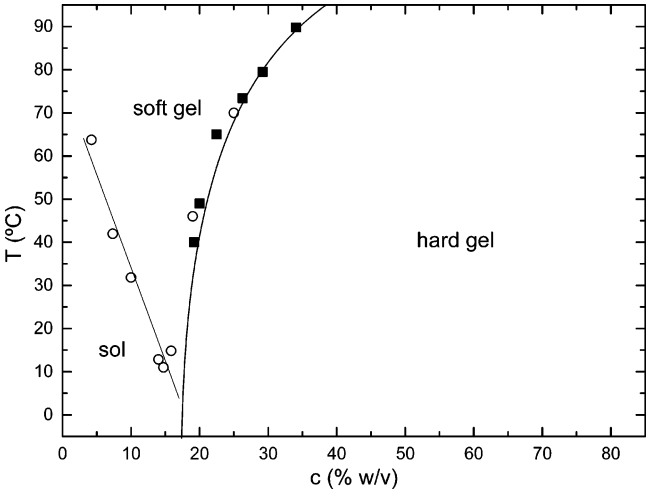

Figure 8. (■) Hard-gel boundary defined by tube inversion and (○) soft-gel and hard-gel boundaries defined by rheometry for aqueous solutions of copolymer $PSO_{10}PEO_{135}$.

the general pattern as those published previously for other PEO/PSO block copolymers.[1,2] The upper limit to the soft gel region for the diblock copolymer is not reached within the temperature range investigated, consistent with the stability at high temperature of the hard gels of this copolymer.

To get a more detailed picture about the rheological behavior of both hard and soft gels, frequency scans of solution of both block copolymers were performed. Examples of soft gels are shown in Figure 9: Figure 9a shows the frequency scan obtained for the 16% (w/v) solution of copolymer $PSO_{10}PEO_{135}$ at 45 °C. This soft gel at temperatures and concentrations relatively near the hard-gel boundary can be assigned as defective versions of the cubic packed hard gels, i.e., small structured domains in an overall fluid matrix. Soft gels of this type have been also studied for PEO-PBO copolymers using SAXS[50] and. for low-T aqueous soft gel of Pluronic F127 using SANS.[51] Comparison may be established with Figure 9b, where a frequency scan for a 40% (w/v) hard gel of copolymer $PSO_{10}PEO_{135}$ at 45 °C is depicted. The high values of the storage modulus ($G' \approx 10$ kPa at $f = 1$ Hz) in the linear viscoelastic region, the almost constant value of log G', and the minimum in log G'' are all characteristic of a hard gel formed by cubic packing of spherical micelles[52] These features are also seen in microphase-separated block copolymer melts with centered cubic structures[53] and in those of colloidal hard spheres near the fluid−solid transition.[54] Although the modulus values are low ($G' \approx 100$ Pa and $G'' \approx 30$ Pa at $f = 1$ Hz, $A = 0.5\%$) compared to those of the hard gel, log G' is approaching a constant value, while log G'' also shows a shallow minimum, and both moduli do not show a crossover point in the measured frequency range.

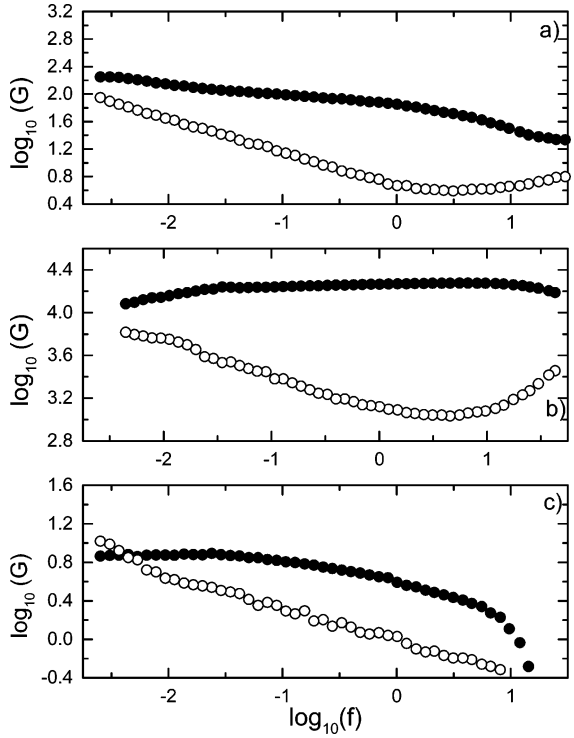

Figure 9. Frequency dependence of (●) storage and (○) loss modulus (log−log plot) for (a) 16% (w/v) aqueous solution of copolymer PSO_{10}-PEO_{135} in soft-gel region, (b) 40% (w/v) aqueous gel of copolymer $PSO_{10}PEO_{135}$ in hard-gel region. $T = 45$ °C and strain amplitude $A = 0.5\%$; (c) 7% (w/v) aqueous solution of copolymer $PSO_{10}PEO_{135}$ in soft gel region at $T = 60$ °C.

On the other hand, the scan obtained for a 7% (w/v) solution at 60 °C differs (see Figure 9c) from that of Figure 9a, having very low values of G' (e.g. $G' \approx 75$ Pa at f = 1 Hz, A = 0.5%), and with indications of a moduli crossover at low frequency, corresponding to a Maxwell fluid, at most, showing localized cubic order. This must be a consequence of the weak attraction of spherical micelles in water at temperatures where it is a poor solvent for the micelles. The transition from sol to soft gel may well occur when aggregates of spherical micelles reach the percolation threshold yielding sufficient structure to cause the characteristic rheological effect. Soft gels of this type have been also identified in aqueous micellar solutions of a wide range of copolymers including other PEO/PSO copolymers,[1,2,52] as well as work on PEO-PPO-PEO copolymers by Hvidt and co-workers who have ascribed the effect in certain systems to the intervention of the sphere-to-rod micellar transition,[36,38] and by Mallamace and co-workers who have identified mechanisms of percolation and packing (structural arrest), depending on temperature and concentration in solutions of copolymer PEO_{13}-$PPO_{30}PEO_{13}$.[55,56]

4. Conclusions

The micellization and gelation properties of two block copolymers with different architecture but similar average hydrophobic block lengths, $S_{10}E_{135}$ and $E_{69}S_8E_{69}$, were studied using surface tension, light scattering, and rheology at different temperatures in both the dilute and concentrated regimes. In particular, the effect of the long hydrophilic block in the diblock architecture was also analyzed and compared to previously structurally related block copolymers of the same type. The values of the cmc at different temperatures obtained by surface tension measurements show that the longer the E-block length, the more hydrophilic the copolymer becomes. It can be observed that the triblock copolymer has a cmc approximately 1 order of magnitude higher than the diblock copolymer. The effect is originated by entropy of the triblock chains constrained by two block junctions in the core interface of the aggregate, compared with only one constraint for the diblock chain. This is confirmed from the calculation of the micellar parameters from light scattering, where the diblock architecture possesses higher radii and association numbers. In addition, light scattering data also show that as temperature increases, the extent of corona hydration decreases as expected, but the level of hydration in the corona remains still important at high temperatures, i.e., the temperature had a very little effect on the hydrodynamic radii as well as on the value of the mass-average association number of the micelles as usually found for block copoly(oxyalkylenes). Tube inversion and rheology measurements provided the phase behavior of both copolymers. From rheology measurements, it was also observed that for a given gel concentration of copolymer, the value of G' increased at low temperatures raises due to an increase in the extent of micellization, whereas G' decreased with increases in the temperature at high temperatures provided that water became a worse solvent for polyoxyethylene, resulting in a compression of the E-block corona and in a decrease in the effective micellar volume fraction in solution. In addition, two different types of soft gels were observed for the diblock structure (studied in more detail as commented on in the text): one at higher polymer concentrations as a result of a defective cubic structure and the other at lower concentrations as a consequences of percolation mechanisms between copolymer micelles acting as hard spheres.

Acknowledgment. The authors thank Ministerio de Ciencia y Tecnología for the research project MAT2007-61604 and Xunta de Galicia for additional financial support. M.A.C. thanks the Pakistan Government for financial support. We thank Profs. Attwood and Booth for a generous gift of block copolymer samples.

References and Notes

(1) Crothers, M.; Attwood, D.; Collet, J. H.; Yang, Z.; Booth, C.; Taboada, P.; Mosquera, V.; Ricardo, N. P. S.; Martini, L. G. A. *Langmuir* **2002**, *18*, 8685−8691.

(2) Yang, Z.; Crothers, M., M.; Ricardo, N. P. S.; Chaibundit, C.; Taboada, P.; Mosquera, V.; Kelarakis, A.; Havredaki, V.; Martini, L.; Valder, C.; Collett, J. H.; Attwood, D.; Heatley, F.; Booth, C. *Langmuir* **2003**, *19*, 943−950.

(3) Kelarakis, A.; Havredaki, V.; Rekatas, C. J.; Booth, C. *Phys. Chem. Chem. Phys*. **2001**, *3*, 5550−5552.

(4) Booth, C.; Attwood, D. *Macromol. Rapid Commun*. **2000**, *21*, 501−527.

(5) Mai, S.-M.; Ludhera, S.; Heatley, F.; Attwood, D.; Booth, C. *J. Chem. Soc., Faraday Trans*. **1998**, *94*, 567−572.

(6) Mai, S.-M., Booth, C.; Kelarakis, A.; Havredaki, V.; Ryan, J. A. *Langmuir* **2000**, *16*, 1681−1688.

(7) Kelarakis, A.; Havredaki, V.; Rekatas, C. J.; Mai, S.-M.; Attwood, D.; Booth, C.; Ryan, A. J.; Hamley, I. W.; Martini, L. G. A. *Macromol. Chem. Phys*. **2001**, *202*, 1345−1354.

(8) Chaibundit, C.; Sumanatrakool, P.; Chinchew, S.; Kanatharana, P.; Tattershall, C. E.; Booth, C.; Yuan, Y.-F. *J. Colloid Interface Sci*. **2005**, *283*, 544−554.

(9) Kelarakis, A.; Havredaki, V.; Viras, K.; Mingvanish, W.; Heatley, F.; Booth, C.; Mai, S.-M. *J. Phys. Chem. B*. **2001**, *105*, 7384−7393.

(10) Mingvanish, W.; Kelarakis, A.; Mai, S.-M.; Daniel, C.; Yang, Z.; Havredaki, W.; Hamley, I. W.; Ryan, A. J.; Booth, C. *J. Phys. Chem. B* **2000**, *104*, 9788−9794.

(11) Lunsted, L. G. *J. Am. Oil Chem. Soc*. **1951**, *28*, 294.

(12) Nace, V. M. *J. Am. Oil Chem. Soc*. **1996**, *73*, 1−8.

(13) Fleute-Schlachter, I. Goldschmidt Industrial Specialties, Essen, Germany. Private communication.

(14) Booth, C.; Attwood, D.; Price, C. *Phys. Chem. Chem. Phys*. **2006**, *8*, 3612−3622.

(15) Rekatas, C. J.; Mai, S.-M.; Cothers, M.; Quinn, M.; Collet, J. H.; Attwood, D.; Heatley, F.; Martini, L. G. A.; Booth, C. *Phys. Chem. Chem. Phys*. **2001**, *3*, 4769−4773.

(16) Crothers, M.; Zhou, Z.; Ricardo, N. P. S.; Yang, Z.; Taboada, P.; Chaibundit, C.; Attwood, D.; Booth, C. *Int. J. Pharm*. **2005**, *293*, 91−100.

(17) Provencher, S. W. *Makromol. Chem*. **1979**, 180 201−209.

(18) El-Kashef, H. *Rev. Sci. Instrum.* **1998**, *69*, 1243−1245. Liu, T.; Schuch, H.; Gerst, M.; Chu, B. *Macromolecules* **1999**, *32*, 6031−6042. The temperature dependence of the Raleigh ratio was not found in the literature and, as a working approximation, values of R_V for toluene were adjusted relative to those published for benzene: Gulari, E.; Chu, B.; Liu, T. Y. *Biopolymers* **1979**, *18*, 2943. The adjustment is small over the temperature range involved.

(19) Percus, J. K.; Yevick, G. J. *J. Phys. Rev.* **1958**, *110*, 1−13. Vrij, A. *J. Chem. Phys*. **1978**, *69*, 1742−1747. Carnahan, N. F.; Starling, K. E. *J. Chem. Phys.* **1969**, *51*, 635−636.

(20) Mai, S.-M.; Booth, C.; Nace, V. M. *Eur. Polym J*. **1997**, *33*, 991−996. Kern, R. J. *Makromol. Chem*. **1965**, *81*, 261−263.

(21) Reddy, N. K.; Foster, A.; Styring, M. G.; Booth, C. *J. Colloid Interface Sci*. **1990**, *136*, 588−593.

(22) Taboada, P.; Velasquez, G.; Barbosa, S.; Castelletto, V.; Nixon, S. K. Z.; Heatley, F.; Hamley, I. W.; Ashford, M;, Mosquera, V.; Attwood, D.; Booth, C. *Langmuir* **2005**, *21*, 5263−5271.

(23) Taboada, P.; Velasquez, G.; Barbosa, S.; Yang, Z.; Nixon, S. K; Zhuo, Z.; Heatley, F.; Ashford, M.; V. Mosquera, V.; Attwood, D.; Booth, C. *Langmuir* **2006**, *22* 7465−7470.

(24) Chu, B. *Langmuir* **1995**, *11*, 414−521. Yuan, X.-F.; Masters, A. J.; Price, C. *Macromolecules* **1992**, *25*, 6876−6884.

(25) Hall, D. G. In *Nonionic Surfactants. Physical Chemistry*, Vol. 23; Schick, M. J., Ed.; Decker: New York, 1987; p 247.

(26) Taboada, P.; Mosquera, V.; Attwood, D.; Yang, Z.; Booth, C. *Phys. Chem. Chem. Phys*. **2003**, *5*, 2625−2627.

(27) Hiemenz, P. C.; Rajahgopalan, R. *Principles of Colloid and Surface Chemistry*; Dekker: New York, 1997.

(28) Kelarakis, A.; Havredaki, V.; Yu, G.-E.; Derici, L.; Booth, C.; *Macromolecules* **1998**, *31*, 944−946.

(29) Sony, S. S.; Sastry, N. V.; George, J.; Bohidar, H. B. *Langmuir* **2003**, *19*, 4597−4603.

(30) Chu, B.; Zhou, Z. K. In *Nonionic Surfactants, Poly(oxyalkylene) Block Copolymer;* Surfactant Science Series, Vol. 60; Nace, V. M., Ed.; Dekker: New York, 1996; Chapter 3.

(31) Vink, H. *J. Chem. Soc., Faraday Trans. 1* **1985**, 81, 1725−1730.

(32) Flory P. J. *Principles of Polymer Chemistry*; Cornell University Press: Ithaca, NY, 1953.

(33) (a) Casassa, E. F. In *Polymer Handbook*, 3rd ed.; Brandrup, J., Immergut, E. H., Eds.; Wiley: New York, 1989; p 485. (b) Beattie, W.; Booth, C. *J. Phys. Chem*. **1960**, *64*, 696−697.

(34) Zhou, Z.-K.; Chu, B. *J. Colloid Interface Sci.* **1988**, *126*, 171−180.

(35) Goutev, N.; Nickolov, Z. S.; Georgiev, G.; Matsura, H. *J. Chem. Soc., Faraday Trans*. **1997**, *93*, 3167−3171.

(36) Hvidt, S.; Jørgensen, E. B.; Brown, W.; Schillén, K. *J. Phys. Chem.* **1994**, *98*, 12320−12328.

(37) Kelarakis, A.; Mingvanish, W.; Daniel, C.; Li, H.; Havredaki, V.; Heatley, F.; Booth, C.; Hamley, I. W. *Phys. Chem. Chem. Phys*. **2000**, *2*, 2755−2763.

(38) Algrem, M.; Brown, W.; Hvidt, S. *Colloid Polym. Sci.* **1995**, *273*, 2−15.

(39) Hamley, I. W.; Daniel, C.; Mingvanish, W.; Mai, S.-M.; Booth, C.; Messe, L.; Ryan, A. J. *Langmuir* **2000**, *16*, 2508−2514.

(40) Chaibundit, C.; Mai, S.-M.; Heatley, F.; Booth, C. *Langmuir* **2000**, *16*, 9645−9652.

(41) Wanka, G.; Hoffmann, H.; Ulbritch, W. *Macromolecules* **1994**, *27*, 4145−4159.

(42) Yang, Y. -W.; Ali-Adib, Z.; McKeown, N. B.; Ryan, A. J.; Attwood, D.; Booth, C. *Langmuir* **1997**, *13*, 1860−1861.

(43) Castelletto, V.; Hamley, I. W.; Crothers, C.; Attwood, D.; Yang, Z.; Booth, C. *J. Macromol. Sci., Phys.* **2004**, *43*, 13−27.

(44) Mortensen, K.; Brown, W. *Macromolecules* **1993**, *26*, 4128−4135.

(45) Derici, L.; Ledger, S.; Mai, S.-M.; Booth, C.; Hamley, I. W.; Pedersen, J. S. *Phys. Chem. Chem. Phys*. **1999**, *1*, 2773−2785.

(46) Castelletto, V.; Hamley, I. W.; Holmsquit, P.; Rekatas, C. J.; Booth, C.; Grossmann, J. G. *Colloid Polym. Sci.* **2001**, *279*, 621−628.

(47) Hamley, I. W.; Mai, S.-M.; Ryan, A. J.; Fairclough, J. P. A.; Booth, C. *Phys. Chem. Chem. Phys*. **2001**, *3*, 2972−2980.

(48) Bedells, A. D.; Arafeh, R. M.; Yang, Z.; Attwood, D.; Padget, J.; Price, C.; Booth, C. *J. Chem. Soc., Faraday Trans*. **1993**, *89*, 1243−1247.

(49) Kelarakis, A.; Havredaki, V.; Yuan, X.-F.; Chaibundit, C.; Booth, C. *Macromol. Chem. Phys*. **2006**, *207*, 903−909.

(50) Castelletto, V.; Caillet, C.; Fundin, J.; Hamley, I. W.; Yang, Z.; Kelarakis, A. *J. Chem Phys.* **2002**, *116*, 10947−10958.

(51) Prud'homme, R. K.; Wu, G.; Schneider, D. K. *Langmuir* **1996**, *12*, 4651−4659.

(52) Li, H.; Yu, G.-E.; Price, C.; Booth, C.; Fairclough, J. P. A.; Ryan, A. J.; Mortensen, K. *Langmuir* **2003**, *19*, 1075−1081.

(53) Kelarakis, A.; Yuan, X.-F.; Mai, S.-M.; Yang, Y. W.; Booth, C. *Phys. Chem. Chem. Phys*. **2003**, *5*, 2628−2634.

(54) Zhao, J.; Majumdar, B.; Schulz, M. F.; Bates, F. S.; Almdal, K.; Mortensen, K.; Hadjuk, D. A.; Gruner, S. M. *Macromolecules* **1996**, *29*, 1204−1215.

(55) Lobry, L.; Micali, N.; Mallamace, M.; Liao, C.; Chen, S. H. *Phys. Rev. E* **1999**, *60*, 7076−7087.

(56) Chen, S. H.; Chen, W. R.; Mallamace, F. *Science* **2003**, *300*, 619−622.